2019

The simultaneous mitigation of slow and fast voltage fluctuations caused by rooftop solar PV by controlling the charging/ discharging of an integrated battery energy storage system

Prabha Ariyaratna
University of Wollongong, pma072@uowmail.edu.au

Kashem M. Muttaqi
University of Wollongong, kashem@uow.edu.au

Danny Sutanto
University of Wollongong, soetanto@uow.edu.au

The simultaneous mitigation of slow and fast voltage fluctuations caused by rooftop solar PV by controlling the charging/discharging of an integrated battery energy storage system

Abstract

Both slow and fast voltage fluctuations in the connected low voltage (LV) distribution feeder are caused by intermittent variations in solar PV power output, in addition to the variations in load demand where rooftop solar photo-voltaic (PV) unit penetration is higher. A single energy storage system integrated with the solar PV unit can mitigate these fluctuations in voltage profile. A novel analytical approach to mitigate both slow and fast voltage fluctuations simultaneously in the connected LV distribution feeder is proposed, which has not explicitly been addressed in the literature. Integrated battery energy storage systems will be dynamically charged during mid-day to alleviate the voltage rise and discharged during the evening peak hours to alleviate the voltage drop, while simultaneously controlling the fast fluctuations of the PV inverter output to a specified value. The proposed control strategy has been validated using a hypothetical distribution feeder system and results have demonstrated that both the slow and the fast voltage fluctuations in the voltage profile can effectively be alleviated, if the proposed strategy is implemented.

Disciplines

Engineering | Science and Technology Studies

Publication Details

P. M. Ariyaratna, K. M. Muttaqi & D. Sutanto, "The simultaneous mitigation of slow and fast voltage fluctuations caused by rooftop solar PV by controlling the charging/discharging of an integrated battery energy storage system," Journal of Energy Storage, vol. 26, pp. 100971-1-100971-11, 2019.

The Simultaneous Mitigation of Slow and Fast Voltage Fluctuations Caused by Rooftop Solar PV by Controlling the Charging/Discharging of an Integrated Battery Energy Storage System

Prabha M Ariyaratna, Kashem M Muttaqi*, Danny Sutanto

Australian Power Quality and Reliability Centre, School of Electrical, Computer and Telecommunications Engineering, University of Wollongong, Wollongong, NSW 2522, Australia
kashem@uow.edu.au

Abstract: Both slow and fast voltage fluctuations in the connected low voltage (LV) distribution feeder are caused by intermittent variations in solar PV power output, in addition to the variations in load demand where rooftop solar photo-voltaic (PV) unit penetration is higher. A single energy storage system integrated with the solar PV unit can mitigate these fluctuations in voltage profile. A novel analytical approach to mitigate both slow and fast voltage fluctuations simultaneously in the connected LV distribution feeder is proposed, which has not explicitly been addressed in the literature. Integrated battery energy storage systems will be dynamically charged during mid-day to alleviate the voltage rise and discharged during the evening peak hours to alleviate the voltage drop, while simultaneously controlling the fast fluctuations of the PV inverter output to a specified value. The proposed control strategy has been validated using a hypothetical distribution feeder system and results have demonstrated that both the slow and the fast voltage fluctuations in the voltage profile can effectively be alleviated, if the proposed strategy is implemented.

1. Introduction

The deployment of rooftop solar PV units in household and commercial customers has been accelerated during past few years. The introduction of the government and the retailer incentive schemes has caused the increase in the popularity. A high penetration of the rooftop solar PV units in weak power distribution networks can cause voltage drop during the peak demand period and voltage rise during the peak generation period in the voltage profile of the connected distribution feeder. In addition, the events of cloud passing over the rooftop solar PV unit may cause sudden voltage fluctuation in the voltage profile at the connected power distribution feeder. Therefore, the limit of operating voltage may be violated which is variable based on the penetration level of solar PV units. As a result, the distribution network operators (DNO) have enforced limitations on the penetration levels of rooftop solar PV units connected to the distribution feeder as a precaution to avoid/delay expensive grid upgrades [1]. Therefore, it is essential to exploit the limitation on penetration levels by introducing appropriate control mechanism/s to maintain the operating voltage limits in the power distribution feeder.

In general, the slow fluctuations (SF) in the voltage profile are caused by the variation of sun irradiation and the load demand. The fast fluctuations (FF) in the voltage profile are caused by the cloud passing. A case study to show the advantage of having residential rooftop solar PV units integrated with Battery Energy Storage System (BESS) over industrial scale solar farms has been discussed in [2], while highlighting economic and environmental benefits of the rooftop solar PV units. Strategies for voltage regulation and peak shaving with BESS are discussed in [1], with one of the objectives is to reduce the annual cost. The peak shaving with BESS based on the load data is discussed in [3]. A load shifting mechanism from peak hours to off-peak hours is addressed with the utilisation of BESS in [4]. However, both

methods in [3-4] could be improved further by considering the voltage level of the distribution feeder as a minimum requirement to activate peak shaving/load shifting. A dynamic state analysis on the subject of the voltage regulation was carried out in [5], however, the State of Charge (SoC) of the BESS has not been measured as the limiting factor. Also, a voltage-based storage control is discussed for distributed solar PV generation with battery systems in [6]. The paper in [6] proposes the regulation of voltage to mitigate the slow fluctuation in the PV generation. However, the paper has not considered practical issues such as the limited BESS capacity, the sudden fluctuations in the PV generation, etc. The active and reactive power control to alleviate the over-voltage limit violation is studied in [7] using the most recent previous 15 second PV output to forecast the curtailment threshold. The proposed control strategy has been shown to be unsuccessful in the presence of sudden large fluctuations in the PV output. A mechanism to control the BESS SoC, while controlling the slow and fast fluctuation in the voltage profile, is proposed in [8 - 9]. However, the results show that the reverse power flow is minimized rather than avoided. A droop based control mechanism on distributed BESS SoC is discussed for a slow voltage fluctuation control in the distribution feeder in [10 - 11], specifically to avoid the violation of the limit of SoC. However, both [10 – 11] discuss the requirement of the establishment of prior communication between all the distributed BESS to accomplish the application of the control strategy. A multi-level inverter that is integrated with a solar PV generator and BESS is discussed in [12], showing the successful results for a short time period, and has suggested that the studies could be extended further by analysing results for a longer time (24 hour) period. An ESS control mechanism to alleviate the sudden fluctuations in the voltage profile is discussed in [13-14]. However, the authors have not considered avoiding/reducing the reverse power flow to the grid and controlling the voltage in the feeder.

The necessity to investigate a smart way to mitigate both slow and first voltage fluctuations mitigation that considers practical issues such as the limited BESS capacity, the sudden fluctuations in the PV generation with high ramp rate, and the SoC limits motivates us to carry out the research in [15]. The slow and fast fluctuation mitigation in the voltage profile of the connected distribution feeder of the rooftop solar PV using a hybrid energy storage system was developed by the authors and presented in [16]. To mitigate both slow and fast fluctuations in the voltage profile simultaneously, the size and the capacity of the BESS were determined by the authors in [17] based on the 24-hour availability of BESS.

In this paper, the simultaneous operation of the slow and fast voltage fluctuations control (SFVFC) will be explored in the context of solar PV units in LV distribution feeders. The proposed approach utilizes a single battery energy storage system (BESS) to be integrated with the PV unit for this purpose, which will be dynamically charged during mid-day to alleviate the voltage rise and discharged during the evening peak hours to alleviate the voltage drop, while simultaneously controlling the fluctuations of the PV output. This also controls the voltage levels during both FF and SF by using a BESS whilst managing BESS SoC dynamically to provide necessary control throughout the day. The methodology will be simulated on a hypothetical distribution feeder system based on 24 hour and 7 day data in 1 second intervals.

2. **Available Control Techniques to Control Rate of Change of Solar PV Inverter Output**

The various techniques to control the rate of change of solar PV inverter output based on the input or sequential inputs of the solar PV generator have been discussed in the

literature [18-25]. A comparison of the reported techniques in the literature is shown in Table 1.

Table 1: Comparison of Control Techniques in literature

Method	***Ref.***	***Technical Criteria***			
		Effectiveness of storage time	***Losses in storage system***	***SOC level***	***Cycling degradation***
Ramp rate control	[20], [21]	Very Good	Average	Maintain 40-60% often	Less than 2% always
Moving Average	[21], [23], [24], [25]	Bad	High	Vary between 0-100% letting 0-10% frequent	Approximately 10% for 0W-40kW solar panels
Step Control	[21]	Good	Low	Maintain 40-60% often	Less than 1% always
Low pass flilter	[23], [22]	Bad	Low	Maintain 60-90%often	Very low as 0.5% always
Moving median	[24]	Bad	High	Vary between 0-100%, including rapid	Approximately 10%

The rate of change of the inverter output is maintained at a specified rate in [20]. Few variables are required determination to avoid the energy loss of PV generation caused by the BESS output which always depends on the previous BESS output. The ramp rate control in [21] is based on the percentage change of ramp rate with respect to the PV generation, which makes the method inefficient. The moving average method and its adaptations such as the lagging moving average, the cantered moving average, etc. have been discussed in [20, 23-25], and the results depends on the selection of the time window, which deliver less desirable results due to higher dependency on previous generation data.

The low pass filter method has been studied in [22-23]. When the ramp rate is limited to less than 5%/min, the requirement for the capacity of the storage system drastically increases [22]. The lagging and double moving average methods produce different results based on the size of window and the solar PV output data [23-24]. The double moving average method produces a smoother output compared with other moving average methods.

The methodology proposed in this research for the mitigation of FF in the voltage profile does not depend on a time window. Therefore, it can have the ability to control the

output based on the present power output of the PV generator and a specified maximum rate of change, which is a novel technique Introduced by authors in [15].

3. The Proposed Methodology to Alleviate the Slow and Fast Fluctuation in Voltage Profile Using BESS

The proposed simultaneous voltage control proposes to mitigate both the slow and the fast fluctuations caused by the mismatch between the solar PV output and the residential load will be achieved. The conceptual block diagram of a typical BS integrated with a rooftop solar PV system, which will be studied in this work, is presented in Fig. 1.

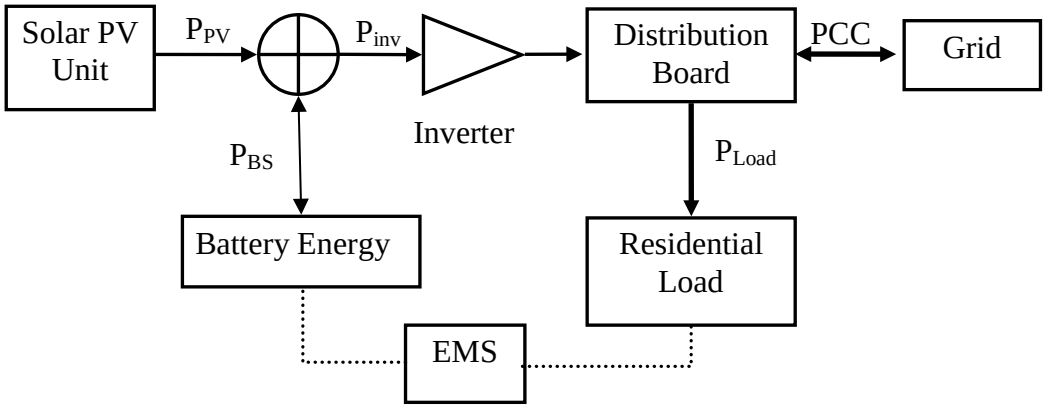

Figure 1: Conceptual Diagram of the solar PV unit with BESS

The BS will be charged/discharged faster to mitigate the fast fluctuations in the solar PV output (FF_{PV}) and charged/discharged slower to mitigate the slow fluctuations in the voltage level at the PCC (SF_{PCC}). Both controller mechanisms will be integrated to operate using a single BS within its technical limitations. As per Fig. 1, the solar PV unit and the BS are connected through an inverter to the residential load and the grid. Firstly, the BS power output to mitigate FF_{PV} will be calculated. The BS power output to compensate SF_{PCC} will be calculated next and then the BS will be operated to mitigate both fast and slow fluctuations simultaneously. It is assumed that the communication within the Energy Management System (EMS) does not experience any delay in the response time.

The power output from the solar panel (P_{PV}) and the power injection/absorption to/from grid (P_{Grid}) must be equal to the power output of the BESS (P_{BESS}) and the load demand (P_{Load}), as shown as Eq.1 below,

$$P_{PV} + P_{Grid} = P_{Load} + P_{BESS} \quad (1)$$

The regulation of P_{Grid} by controlling P_{BESS} is essential to maintain the voltage profile within the standard operating limit within the standard operating limit of the connected power distribution feeder. However, it is assumed the BESS has a sufficient capacity to deal with the power requirement (P_{BESS}) for the proposed SFVFC.

An illustration of the Eq. 1 is depicted in Fig. 2, which contains a hypothetical data (in watts) for analysis.

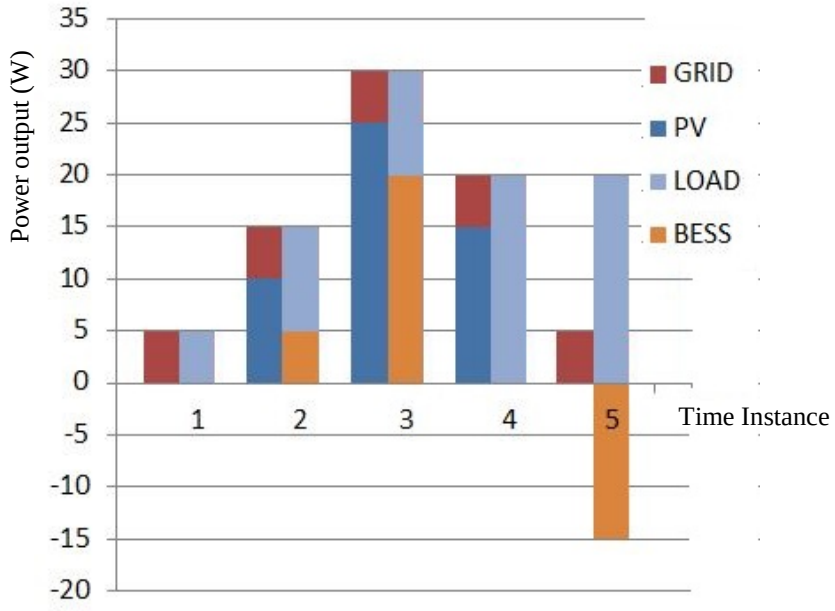

Figure 2: Power outputs of solar PV, BESS, load demand and power absorption from grid

The power absorption from the grid, (P_{Grid}), is considered unchanged for the ease of analysis. At the 1st instance, P_{PV} is null, P_{BESS} is null, load demand is supplied by the grid and hence, P_{Grid} is equivalent to P_{Load}. During 2nd and 3rd instances, P_{PV} is 10W and 25W respectively, P_{BESS} is 5W and 20W, P_{Load} is 10W in both instances, required 5W (P_{Grid})is supplied by the grid. At the 4th instance, P_{PV} is 10W, P_{Load} is 15W, P_{BESS} is null and P_{Grid} is 5W. In the 5th instance, P_{PV} is null, P_{Load} is 20W, P_{BESS} is discharging 15W and P_{Grid} is 5W.

3.1 Alleviation of the Fast Fluctuations (FF) in the voltage profile

The FF in the voltage profile is caused by the cloud passing over the solar PV unit. The maximum allowable rapid voltage change of LV network is 5% under normal circumstances and 10% if it is infrequent, based on the EN50160 standard for voltage disturbances [19].

The output of the integrated BESS and the PV inverter, $P_{inv,}$ can be obtained as an expression of the PV panel output power, $P_{PV,}$ the inverter efficiency, η_{inv} and the battery output power, $P_{BESS,}$ as given below [15]:

$$P_{inv} = \eta_{inv} \times (P_{PV} + P_{BESS}) \quad (2)$$

After differentiating all the terms in (2), and rearranging, we obtain (3),

$$\frac{dP_{BESS}}{dt} = \frac{1}{\eta_{inv}} \left[\frac{dP_{inv}}{dt}\bigg|_{def} - \eta_{inv} \times \frac{dP_{PV}}{dt} \right] \quad (3)$$

The rate of change of the solar PV output, $\frac{dP_{PV}}{dt}$, is referred to as the solar PV ramp rate (PVRR). The solar PV inverter efficiency, η_{inv}, can be obtained from the manufacturer data sheet. However, for the calculation here after η_{inv} is considered as unity in value.

The rate of change of the solar PV inverter output is fixed to a specified value and referred as Maximum Applicable Ramp Rate (MARR). The specified ramp rate is set as negative ($MARR_{min}$) when the PVRR is negative and set as positive ($MARR_{max}$) when the PVRR is positive, otherwise, it is set as zero (when PVRR is null), as shown in (4) [15]:

$$MARR = \begin{cases} MARR_{max}, & if \ \frac{dP_{PV}}{dt} > 0 \\ MARR_{min}, & if \ \frac{dP_{PV}}{dt} < 0 \\ 0, & if \ \frac{dP_{PV}}{dt} = 0 \end{cases} \quad (4)$$

The rate of change of the BESS power output, $\frac{dP_{BESS}}{dt}(t)$ can be calculated, after the selection of MARR based on the PVRR of the PV. The rate of change of BESS consists of two parts: the rate of change of BESS during the FF control and the rate of change of BESS during the SF control. This relationship can be shown in (5).

$$\frac{dP_{BESS}}{dt}(t) = \frac{dP_{BESS\_FF}}{dt}(t) + \frac{dP_{BESS\_SF}}{dt}(t) \quad (5)$$

Where, $\frac{dP_{BESS\_FF}}{dt}(t)$ is the rate of change of BESS for the FF control and $\frac{dP_{BESS\_SF}}{dt}(t)$ is the rate of change of BESS for the SF control.

The rate of change of the power output of BESS, $\frac{dP_{BESS\_FF}}{dt}(t)$ can be obtained as below:

$$\frac{dP_{BESS\_FF}}{dt}(t) = \begin{cases} 0, & if \ |PVRR| \leq |MARR| \\ MARR - PVRR, & otherwise \end{cases} \quad (6)$$

As seen in (6), $\frac{dP_{BESS\_FF}}{dt}(t)$ is zero when the absolute value of the current PVRR is equal or lower than the absolute value of the specified MARR. Otherwise, $\frac{dP_{BESS\_FF}}{dt}(t)$ is the gap between MARR and PVRR.

Calculation of $\frac{dP_{BESS\_FF}}{dt}(t)$ based on MARR and PVRR is illustrated in Fig. 3 below using fictions data,

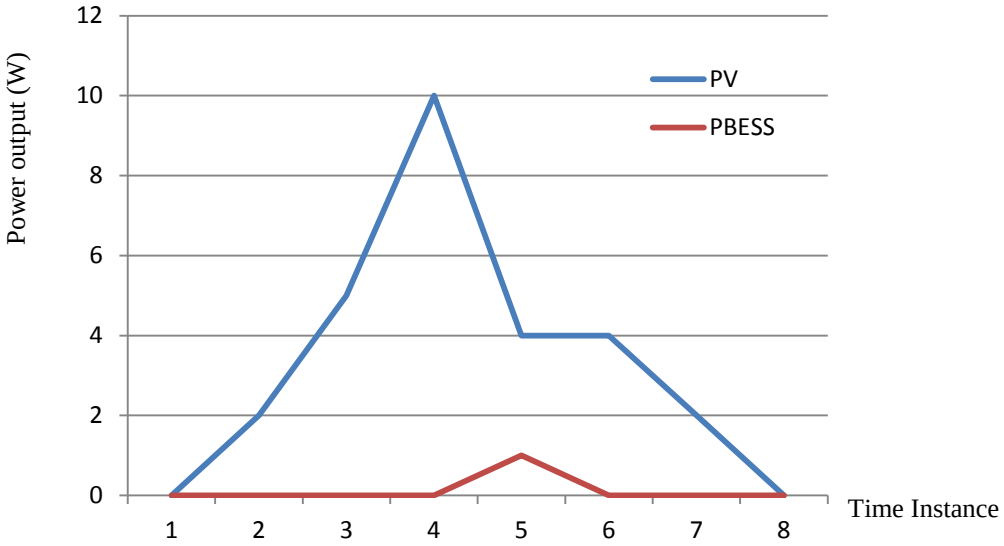

Figure 3 (a): Solar PV data and Battery power output to mitigate fluctuations

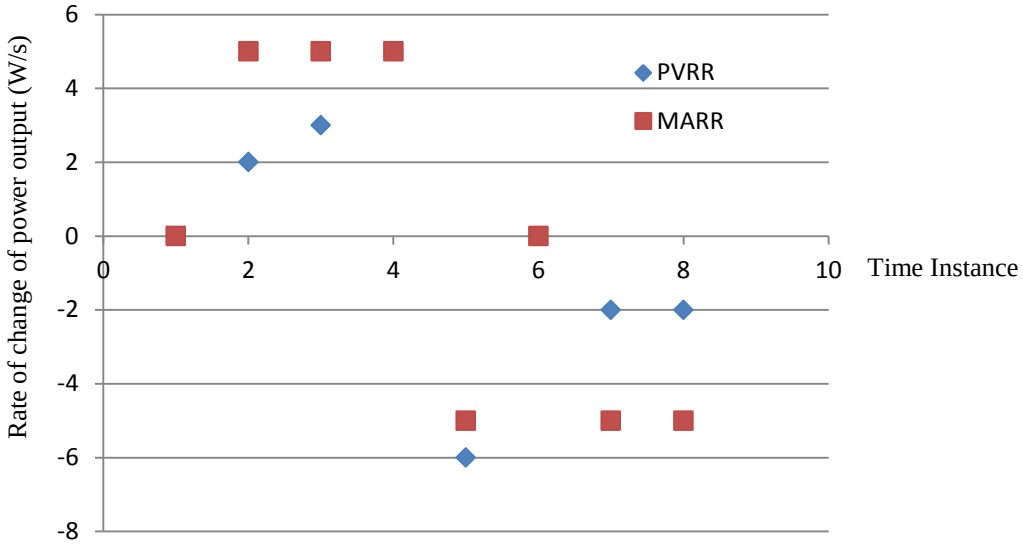

Figure 3 (b): MARR and PVRR

The specified MARR during the illustration was 5W/s. During instance 1 - 2, the solar PV output increased from zero to 2W and hence, the calculated PVRR is 2W/s. However, the PVRR is less than specified MARR, hence, $\frac{dP_{BESS\_FF}}{dt}(t)$ is zero for the duration. During instances 2 - 3 and 3 - 4, the solar PV output increased from 2W to 5W and 5W to 10W respectively. Hence, the calculated PVRR are 3W/s and 5W/s. However, the PVRR is less than specified MARR in both instances and hence, $\frac{dP_{BESS\_FF}}{dt}(t)$ is zero. During instance 4 - 5, the solar PV output decreased from 10W to 4W, the calculated PVRR is -6W/s, which is larger (note that only the absolute values of both PVRR and MARR are compared in (6)) than the specified MARR is -5W/s, hence, the MARR is -5W/s during the duration. Accordingly, $\frac{dP_{BESS\_FF}}{dt}(t)$ is 1W/s. During instance 5 - 6, the solar PV output is stable, and the calculated PVRR is zero. $\frac{dP_{BESS\_FF}}{dt}(t)$ is zero for whole duration, since the PVRR is less than the

MARR. During instances 6 - 7 and 7 - 8, the solar PV output decreased from 4W to 2W and 2W to zero respectively. Hence, the calculated PVRR is -2W/s for both instances. $\frac{dP_{BESS\_FF}}{dt}(t)$ is zero since the PVRR is less than the MARR.

This methodology will be used to calculate $\frac{dP_{BESS\_FF}}{dt}(t)$ for the alleviation of the FF.

3.2 Alleviation of Slow Fluctuations (SF) in the Voltage Profile

The SF in the voltage profile is caused by the changing sun irradiation and insolation against the varying residential load demand. The solar PV generation starts at sunrise and ends at sunset. The imbalance in generation and demand can be balanced using the BESS with a sufficient charge/discharge capacity in BESS.

The ac voltage of the rooftop solar PV should be 230V at the Point of Common Coupling (PCC) in single phase line-to-neutral and 400V in the three phase line- to-line with a tolerance of +10% and -6% [3], according to the Australian Standard AS 60038 for Standard Voltages.

The proposed SF control method dynamically measures the voltage level at PCC to determine the rate of change of charge/discharge rate ($\frac{di_{BESS\_SF}}{dt}(t)$) of BESS. During the methodology to control the SF, several sets of pre-defined voltage levels of PCC is used to determine the rate of change of charge/discharge rate ($\frac{di_{BESS\_SF}}{dt}(t)$) of BESS which is again pre-defined to suit the loading of the feeder. Table 2 contains pre-defined voltage levels and $\frac{di_{BESS\_SF}}{dt}(t)$ for the specific feeder.

Table 2: Method to determine rate of charge/discharge rate of BESS for SF

Lowest reference V_{PCC} Per Unit(P.U)	**Highest reference V_{PCC}(P.U)**	**$\frac{di_{BESS\_SF}}{dt}(t)$ (A/h)**
0.94	1.1	0
BESS Charging to regulate voltage profile		
1.1	1.104	12.5
1.104	1.108	25
1.104	-	50
BESS discharging to regulate voltage profile		
0.93	0.94	25
-	0.92	50

The rate of change of charge/discharge rate of BESS is lower when the voltage at PCC deviates less from the operating voltage range. Similarly, the rate of change of charge/discharge rate of BESS is higher when the voltage at PCC deviates more from the operating voltage range.

A BESS with the capacity of 500Ah is used for the simulations, the rate of change of charging rates ($\frac{\mathrm{di_{BESS\_SF}}}{\mathrm{dt}}$ (t)) are based on 12.5, 25 and 50 A/h respectively. The rate of change of discharging rates ($\frac{\mathrm{di_{BESS\_SF}}}{\mathrm{dt}}$ (t)) are based on 25 and 50A/h.

Once, ($\frac{di_{BESS\_SF}}{dt}(t)$) is determined, the rate of change of BESS power output, $\frac{dP_{BESS\_SF}}{dt}(t)$ can be calculated as in (7).

$$\frac{dP_{BESS\_SF}}{dt}(t) = \frac{\frac{di_{BESS\_SF}}{dt}(t)}{3600} \times V_{BESS} \quad (7)$$

The rate of change of charge/discharge rate in A/h is obtained as per Table 2. The SoC value is the calculated SoC for the previous instance. Both $\frac{di_{BESS\_SF}}{dt}(t)$ value and the SoC value are then used with the battery characteristic curves (Fig. 4) (for 12V lead acid battery curve) [26] to obtain the BESS operating voltage (V_{BESS}) using interpolation. Next, the rate of change of BESS power output, $\frac{dP_{BESS\_SF}}{dt}(t)$ is determined.

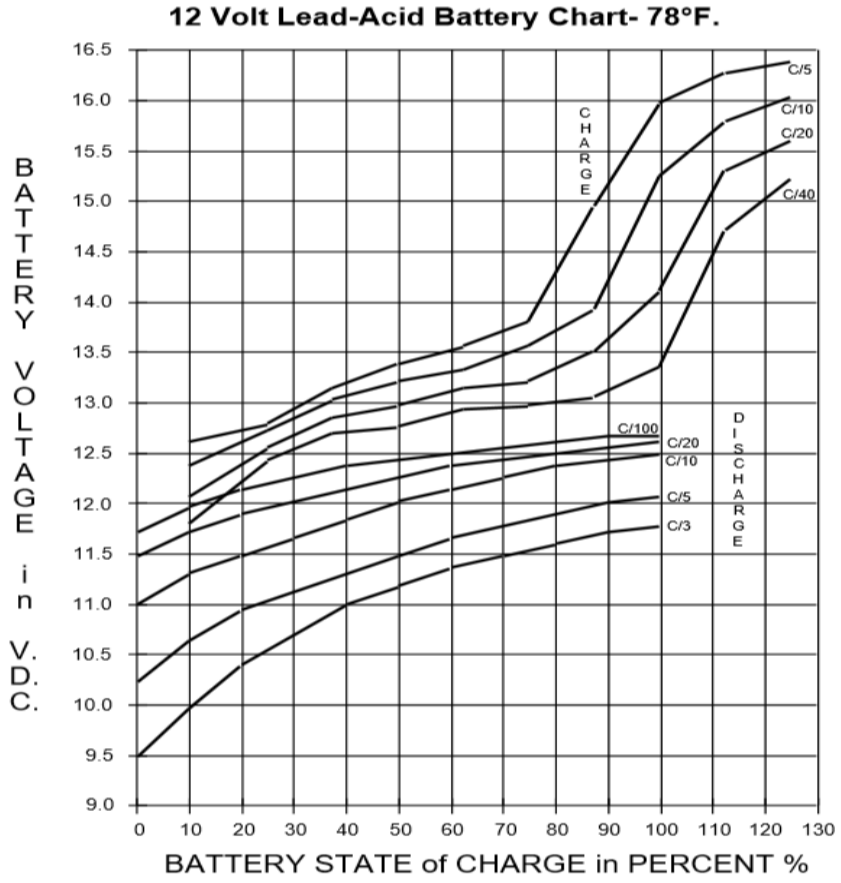

Figure 4: Battery Voltage vs State of Charge (SoC) [26]

3.3 The Tuning of the rate of change of BESS for the alleviation of simultaneous SFVFC

The rate of change of BESS output for FF ($\frac{dP_{BESS\_FF}}{dt}(t)$) and the rate of change of BESS output for SF ($\frac{dP_{BESS\_SF}}{dt}(t)$)are calculated as per Section 3.1 and 3.2 Therefore, according to (5), we have obtained the cumulative rate of change of BESS ($\frac{dP_{BESS}}{dt}(t)$) . Results of calculations are used in (8) for the calculation of the rate of change the inverter output, $\frac{dP_{inv}}{dt}(t)$.

$$\frac{dP_{inv}}{dt}(t) = \frac{dP_{BESS\_FF}}{dt}(t) + \frac{dP_{BESS\_SF}}{dt}(t) + \frac{dP_{PV}}{dt}(t) \quad (8)$$

The calculated $\frac{dP_{inv}}{dt}(t)$ in (8) may exceed the specified MARR value since the cumulative result of the ($\frac{dP_{BESS\_FF}}{dt}(t)$) and the ($\frac{dP_{BESS\_SF}}{dt}(t)$) is used as the rate of change of BESS ($\frac{dP_{BESS}}{dt}(t)$) . The rate of change of BESS ($\frac{dP_{BESS}}{dt}(t)$) should be tuned as shown in (9), if $\frac{dP_{inv}}{dt}(t)$ exceeds the specified MARR value. Otherwise, the control process shall be continued to next step.

$$\frac{dP_{BESS}}{dt}(t) = \frac{dP_{BESS\_FF}}{dt}(t) + \frac{dP_{BESS\_SF}}{dt}(t) =$$
$$= \begin{cases} MARR_{max} - PVRR\ , if\ \frac{dP_{inv}}{dt}(t) > MARR_{max} \\ MARR_{min} - PVRR, if\ \frac{dP_{inv}}{dt}(t) < MARR_{min} \end{cases} \quad (9)$$

The rate of change of the inverter output can be regulated within the specified range of MARR ($MARR_{min}$<MARR< $MARR_{max}$) by tuning the rate of change of BESS ($\frac{dP_{BESS}}{dt}(t)$) according to (9).

If the rate of change of $\frac{dP_{inv}}{dt}$ is higher than $MARR_{max}$ based on the calculation in (8), the rate of change of BESS output should be tuned as to lower $\frac{dP_{inv}}{dt}$ by increasing the rate of change of charging of BESS ($\frac{dP_{BESS}}{dt}(t)$) from the previously calculated value. Accordingly, BESS starts charging at a higher rate and hence the rate of change of inverter output, $\frac{dP_{inv}}{dt}$ is maintained below $MARR_{max}$. If the rate of change of $\frac{dP_{inv}}{dt}$ is lower than $MARR_{min}$ based on the calculation in (8) , the rate of change of BESS should be tuned as to increase $\frac{dP_{inv}}{dt}$ by increasing the rate of change of discharging of BESS ($\frac{dP_{BESS}}{dt}(t)$) from the previously calculated value. Accordingly, BESS starts discharging at a higher rate and hence the rate of change of inverter output, $\frac{dP_{inv}}{dt}$ is maintained above $MARR_{min}$. If the rate of change of $\frac{dP_{inv}}{dt}$ is higher than $MARR_{min}$ and less than $MARR_{max}$ based on the calculation in (8), the rate of change of BESS output does not need to be tuned. Hence, the BESS continues to charge/discharge/idle in similar rate as the previous time instance. The significance of the proposed tuning methodology is the capability to conserve energy throughout the SFVFC to utilize solar energy in the optimum manner.

The command signal is sent to BESS for the generation of the required BESS output, following the calculation of the cumulative rate of charge/discharge of the BESS ($\frac{dP_{BESS}}{dt}(t)$) by tuning,

The power output of BESS for SFVFC, $P_{BESS}(t)$ is calculated based on the cumulative rate of change of charge/discharge of the BESS for the present instance and the power output of BESS for SFVFC in the previous instance which is expressed in (10):

$$P_{BESS}(t) = P_{BESS\_FF}(t) + P_{BESS\_SF}(t) = \begin{cases} 0, & if\ |PVRR| \leq |MARR| \\ P_{BESS}(t-T) + \left[\frac{dP_{BESS\_FF}}{dt}(t) + \frac{dP_{BESS\_SF}}{dt}(t)\right] * \left(t - (t-T)\right), & otherwise \end{cases} \quad (10)$$

The power output of BESS for SFVFC ($P_{BESS}(t)$) is zero when the rate of change of PV (PVRR) is smaller than the specified MARR. In other words, the BESS remain idle when the rate of change of PV (PVRR) is acceptable since PVRR is lower than the maximum acceptable rate of change (MARR). Otherwise, the power output of BESS for SFVFC,($P_{BESS}(t)$) is calculated by applying the amount of change during the selected time duration to the initial $P_{BESS}(t)$ for the previous instance.

3.4 Calculation of the SoC of the BESS

The accumulated Energy of BESS (E_{BESS}) is calculated by intergrating the charged/discharged energy during each time period as in (11),

$$E_{BESS} = \sum_{t=0}^{N} \frac{P_n + P_{n-1}}{2} \times (t_n - t_{n-1}) \quad (11)$$

Where, E_{BESS} is the accumulated energy of BESS, N is the total time duration, P_n is the BESS power output in the present time, P_{n-1} is the BESS power output in the previous time and $t_n - t_{n-1}$ the duration of the selected period.

The SoC of the BESS can be calculated using (12).

$$SoC = \frac{E_{BESS}}{C} \times 100\% \quad (12)$$

Where, SoC is the State of Charge of BESS as a percentage, E_{BESS} is the accumulated energy of BESS and C is the energy capacity of BESS (must be in same units as E_{BESS}).

3.5 Ensuring Undisrupted BESS Availability

Advanced techniques are required to ensure the undisrupted BESS availability to support the SFVFC. The following SoC management techniques are proposed to ensure undisrupted BESS availability throughout the entire duration that require SFVFC. Accordingly, the BESS SoC is enhanced during time periods that BESS is not expected to

perform SFVFC. Consequently, the BESS acquires a sufficient capacity to provide support during upcoming SF and FF in the voltage profile during period that there is no SF or/and FF present in the voltage profile.

Table 3: Method to determine rate of change of charge/discharge rate of BESS for SoC Management

Lowest reference V_{PCC} (P.U)	**Highest reference V_{PCC}(P.U)**	**$\frac{di_{BESS\_SOC}}{dt}(t)$ (A/h)**
BESS Charging for SoC Management		
1.05	1.1	12.5
BESS discharging for SoC Management		
0.945	0.94	12.5

More importantly, the BESS is charged/discharged for SoC management during instances that there is no presence of the SF or/and FF. In addition, if the BESS SoC level is lower than 30% and the V_{PCC} within the lowest and highest reference values for BESS charging as per Table 3, BESS will charge to enhance the SoC. On the other hand, if the BESS SoC level is higher than 90% and the V_{PCC} within the lowest and highest reference values for BESS discharging as per Table 2, BESS will discharge to enhance the SoC. The rate of change of charge/discharge rate ($\frac{di_{BESS\_SOC}}{dt}(t)$) depends on the feeder loading and MARR. In this scenario, $\frac{di_{BESS\_SOC}}{dt}(t)$ will be 12.5 A/h (BESS with 500Ah amphere capacity is used during this work) is for both charging and discharging events to manage SoC.

Once, rate of change of charge/discharge rate, ($\frac{di_{BESS\_SOC}}{dt}(t)$) for SoC management is determined, the rate of change of charge/discharge of BESS, $\frac{dP_{BESS\_SOC}}{dt}(t)$ can be calculated as in (13).

$$\frac{dP_{BESS\_SOC}}{dt}(t) = \frac{\frac{di_{BESS\_SOC}}{dt}(t)}{3600} \times V_{BESS} \quad (13)$$

The rate of change of charge/discharge rate in A/h is obtained as per Table 3 and the SoC is calculated as per (12). Both $\frac{di_{BESS\_SOC}}{dt}(t)$ value and SoC value are then used with the battery characteristic curves (12V lead acid battery curve) [26] to the BESS operating voltage (V_{BESS}) using interpolation. Next, the rate of change of charge/discharge of BESS, $\frac{dP_{BESS\_SOC}}{dt}(t)$ is determined as in (13) for the SoC management.

The controller process should again go through the process to calculate the rate of change of the solar PV output as per discussion presented in Section 3.3.

3.6. Implementation of the Simultaneous Slow and Fast Voltage Fluctuation Control

The detailed methodology of the simultaneous voltage control for the alleviation for slow fluctuations and fast fluctuations in the connected feeder is illustrated in Fig. 5 and elaborated in this section. The methodology is built-in into the BESS which is integrated with the solar PV system.

Initially, the specified MARR value is determined based on the Eq. 4 following the determination of rate of change of solar PV output. Next, the rate of change of BESS output for the control of FF ($\frac{dP_{BESS\_FF}}{dt}(t)$) in voltage profile is determined using Eq. 6.

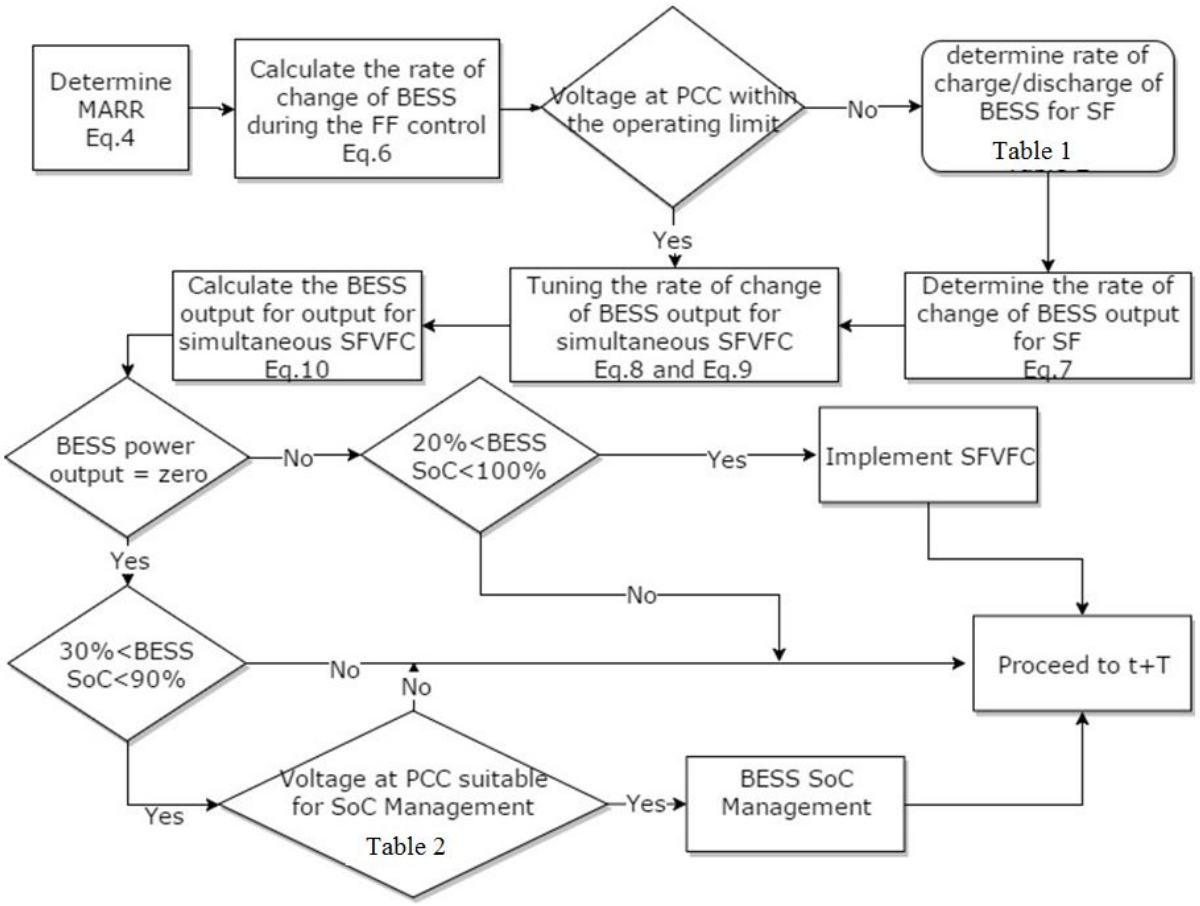

Figure 5: Flow chart for the SFVFC

Thereafter, the voltage at the PCC is determined by applying the load, the BESS output for FF control and the PV output in a quasi-steady-state power flow. Depending on the voltage level at the PCC; the rate of change of charge/discharge rate of BESS ($\frac{di_{BESS\_SF}}{dt}(t)$) is determined using Table 2. Next, the rate of change of BESS power output, $\frac{dP_{BESS\_SF}}{dt}(t)$ is determined using the SoC value from the previous instance and the $\frac{di_{BESS\_SF}}{dt}(t)$ value obtained from the Table 2. The BESS operating voltage (V_{BESS}) is found by the interpolation of BESS characteristics curves to be used in Eq. 7. After the calculation of both $\frac{dP_{BESS\_FF}}{dt}(t)$ and $\frac{dP_{BESS\_SF}}{dt}(t)$, the obtained values are used to tune the BESS output to maintain the rate of

change of the solar PV inverter output within the specifies MARR range, which is performed using Eqs. 8 and 9. The tuned BESS output, $\frac{dP_{BESS}}{dt}(t)$ is used to calculate the BESS power output $P_{BESS}(t)$ using Eq. 10. Accordingly, the BESS power output for the present time instance is calculated using BESS power output of the previous instance and the rate of change of BESS power output for the present instance. However, if the calculated BESS power output is zero, the BESS SoC management may occur depending on the SoC level of the BESS. Accordingly, if the BESS SoC is less than 30% and the voltage at PCC is within range as per Table 2, BESS is charged to increase the SoC above 30%. On the other hand, if the BESS SOC is higher than 90% and the voltage at PCC is within range as per Table 2, BESS is discharged to decrease SoC below 90%. The simultaneous voltage control for slow fluctuations and fast fluctuations is performed, if the calculated BESS power output is not zero and the BESS SoC is within 20-100% SOC range. Finally, the entire operation proceeds to the next time instance.

4. Case Studies

The practical MV/LV system consisting 16 LV buses in the distribution feeder is used to demonstrate the effectiveness of the proposed method described in Section 3. The feeder data for a section of the practical MV/LV network (Fig. 6) in NSW is used. Each bus includes a household with a 5kW rooftop solar PV installed with an integrated 500Ah BESS.

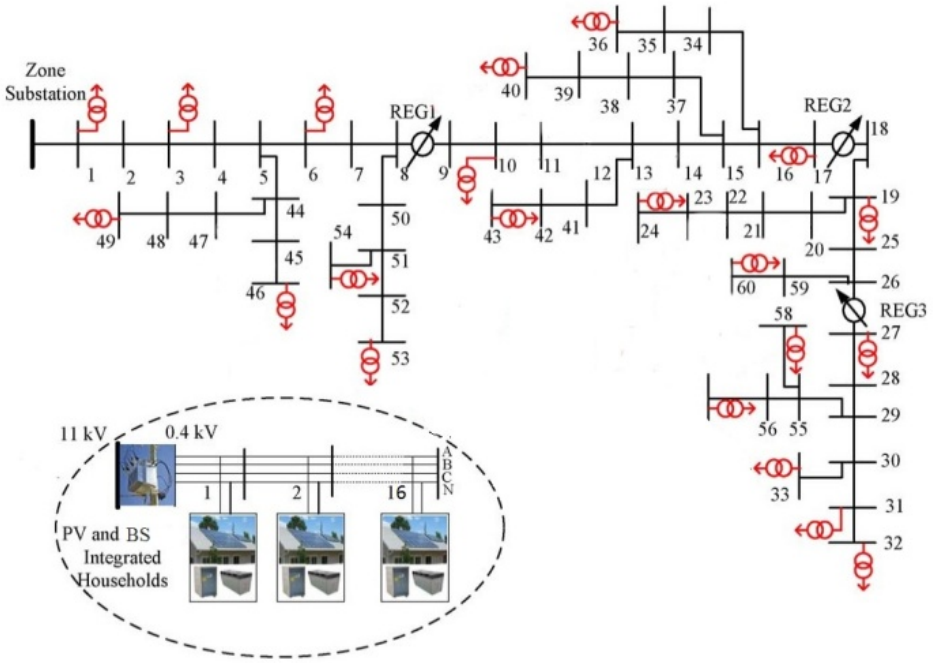

Figure 6: MV/LV Network and the selected LV feeder for simulations

The results will be discussed separately for fast fluctuation control initially and simultaneous slow-fast fluctuation control separately for the advantage of comparison of results to validate the proposed methodology.

Fig. 7, shows the solar PV generation, the BESS power output for FF control and the inverter power output considering the FF control only. The sudden fast fluctuation occurs from 7.30am to 8.15 am and 12.30 pm to 3.30 pm more frequently and vigorously. The

fluctuation with the highest rate of change occurs around 12.30 pm which is roughly 550 Watts/ second.

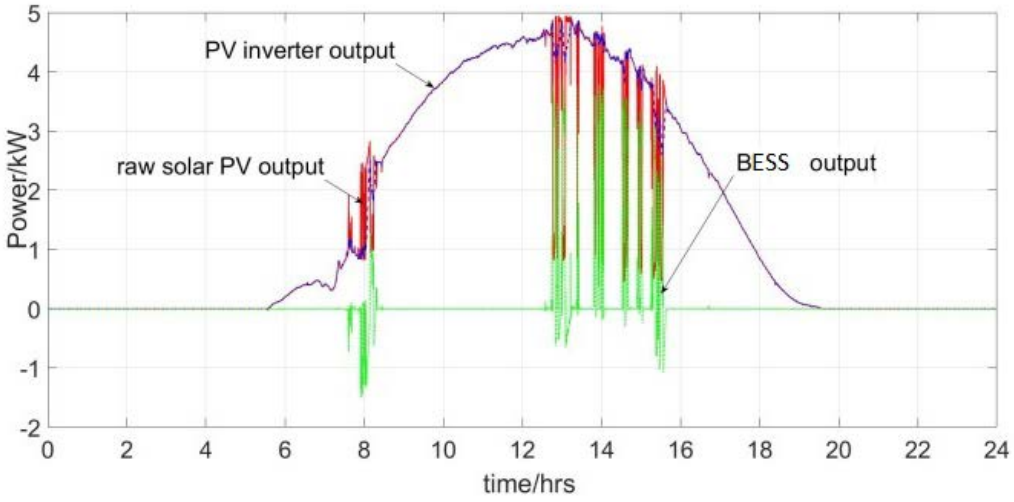

Figure 7: Solar PV generation, BESS power and Inverter power output

Figs. 8 and 9 show the comparison of PVRR and MARR. This resembles the rate of change values with and without FF control. Fig. 9 shows the zoomed 50-second duration of Fig. 8 starting at 12.58.45 hr of the day.

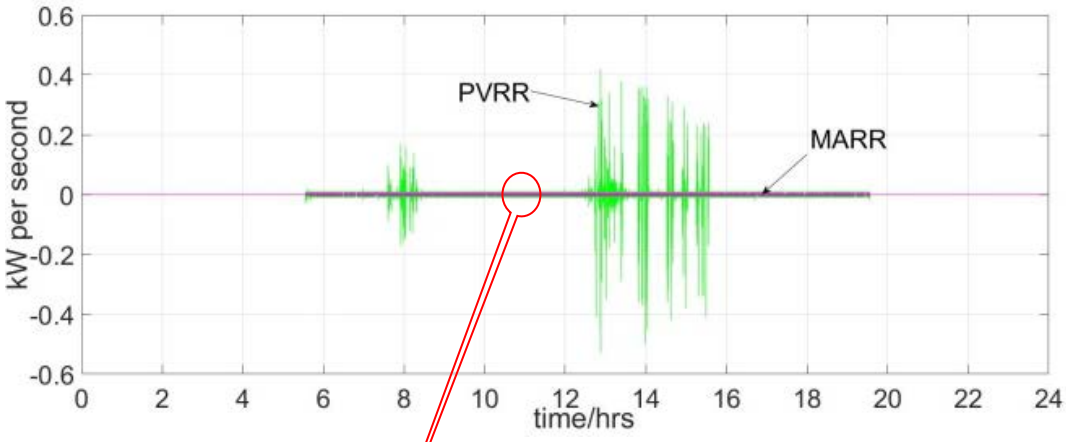

Figure 8: PVRR and MARR

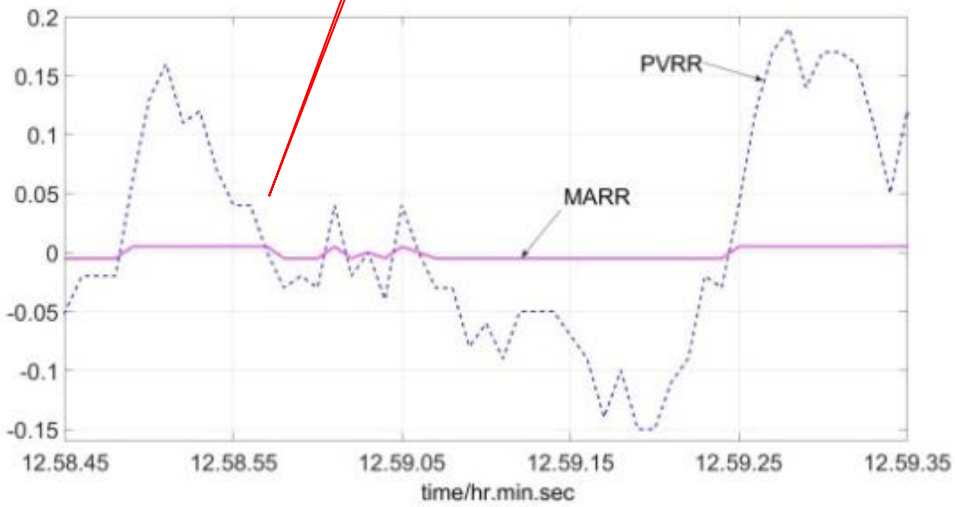

Figure 9: Selected 50 Second duration starting from 12.58.45 hrs in Fig. 8

Fig. 10 shows the battery SoC variation, and approximately 18% of SoC is used for the ramp rate control using a battery with 500Ah capacity. The occurrence of the fast fluctuation events caused the BESS to charge /discharge to maintain MARR.

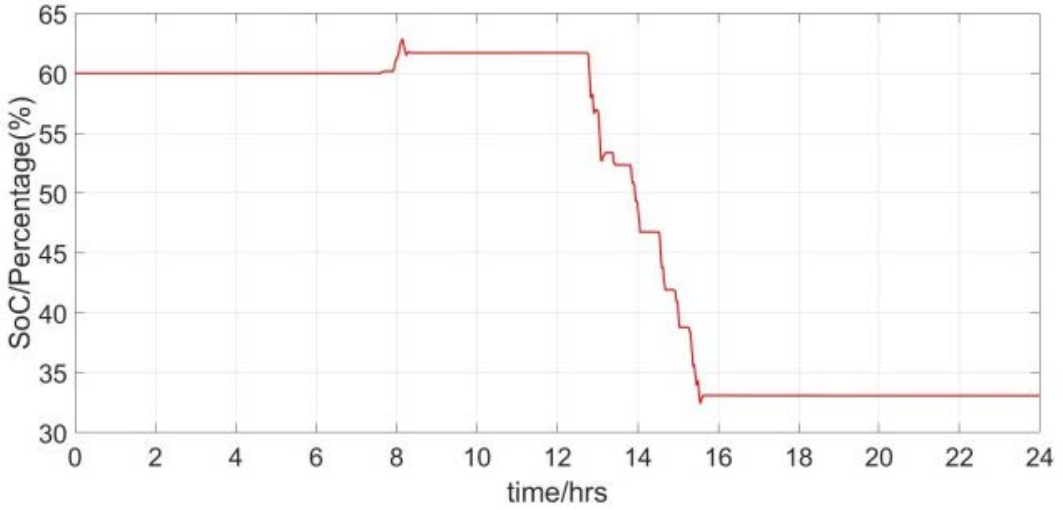

Figure 10: SoC variation considering FF control

Fig. 7 shows the activity level of BESS increases during the passing cloud events resulting in a drop/rise in the SoC level of BESS as shown in Fig. 10 during the same period. With the FF control, the rate of change of the inverter output has been reduced from 550 watts/sec to 5 watts/sec during the highest fluctuation. Similarly, the entire FF with the magnitude over specified MARR have been controlled successfully.

The simulation results for the simultaneous voltage control for both slow fluctuations and fast fluctuations is presented in Figs. 11 - 14 that show the inverter output after the SF control, load data, net power at PCC, BESS SOC variation and voltage profiles for LV bus 16 in the MV/LV network.

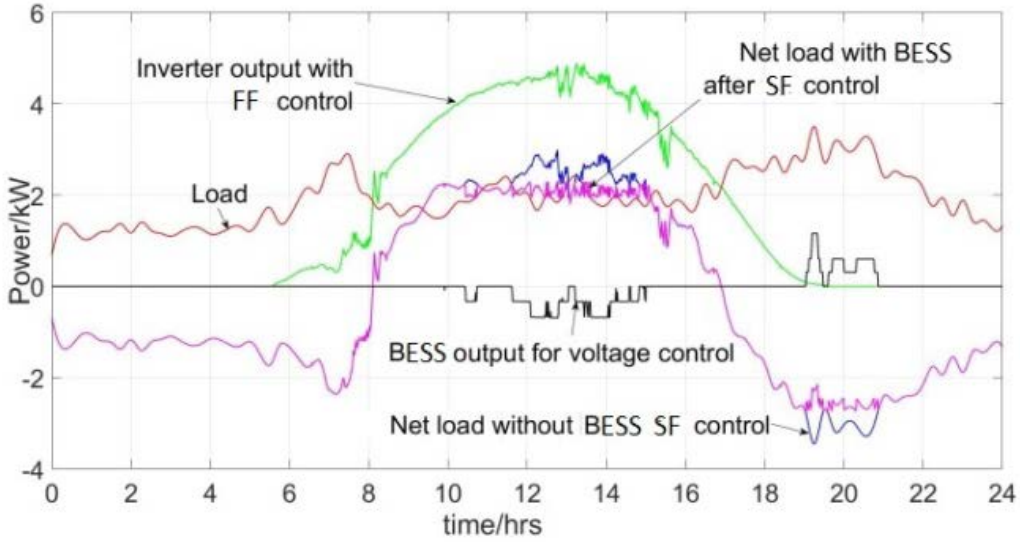

Figure 11: Inverter output, load demand, net power with/without BESS for FF control

Fig. 11 depicts the inverter output after the simultaneous control, the load demand, the BESS power output for voltage control and the net power with/without BESS for voltage control. The BESS is charged in three different charging rates depending on the voltage at PCC during mid-day. As a result, the voltage profile is maintained stable close to the

operating voltage limit. The BESS is discharged in three different charging rates during the evening. The BESS starts charging from 10am until 3 pm, and discharges from around 7pm until 9pm for voltage control.

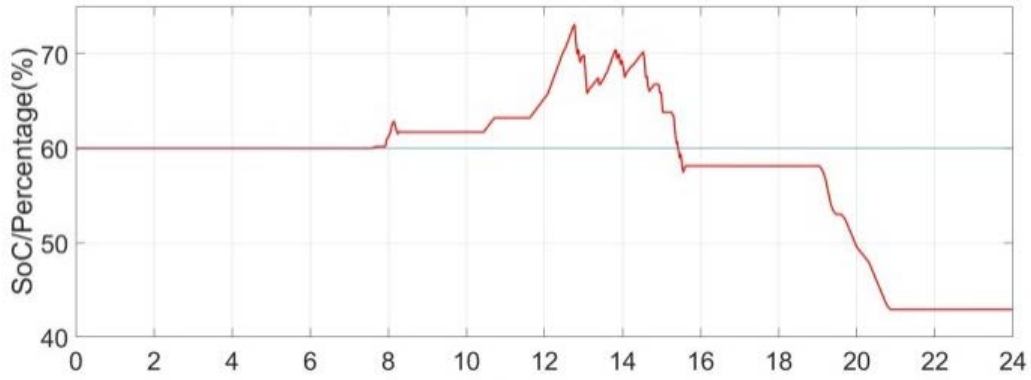

Figure 12: BESS SOC

Fig. 12 depicts the variation of the BESS SoC for the integrated control. The BESS SoC has started from 60% SoC and ended to be 42% SoC by the end of the day after carrying out the simultaneous SFVFC.

Fig. 13 shows the voltage profile without any control at PCC of the 16th LV bus in the test feeder. Fig. 14 depicts the voltage profile with FF control and voltage profile with SFVFC. Accordingly, sudden fast fluctuations in the Fig. 13 have been successfully alleviated as per the illustration in Fig. 14 with the proposed SFVFC technique. Moreover, voltage profile has been successfully controlled within the operating voltage range with the suggested voltage control mechanism.

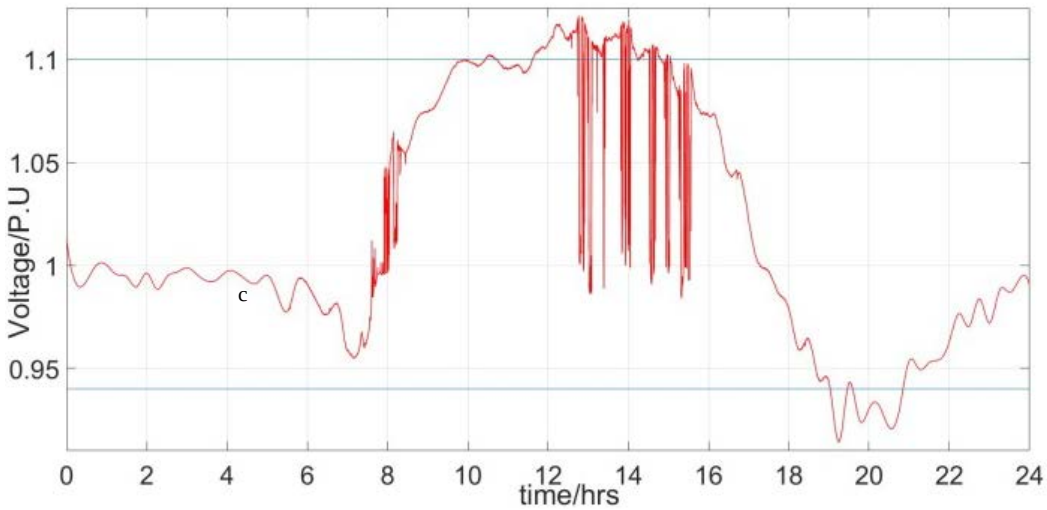

Figure 13: Voltage profile without control

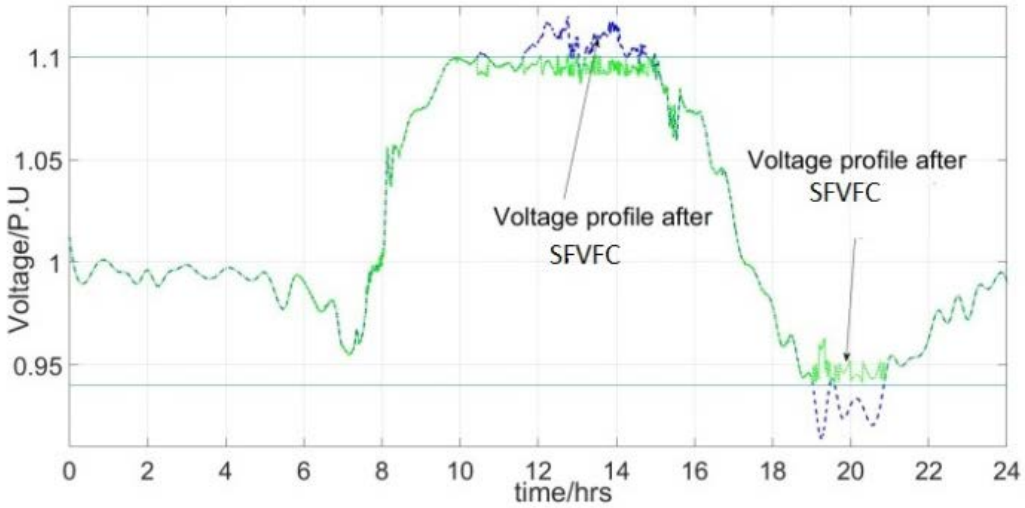

Figure. 14: Voltage profile with FF control only and SFVFC

Moreover, the proposed simultaneous SFVFC was tested together with the SoC management technique on the same feeder considering 7 day data set to validate the hypothesis comprehensively. Fig. 15- Fig. 18 illustrates the inverter output, BESS power output, SoC variation, voltage improvement with FF control and with simultaneous SFVFC for a week starting from Monday.

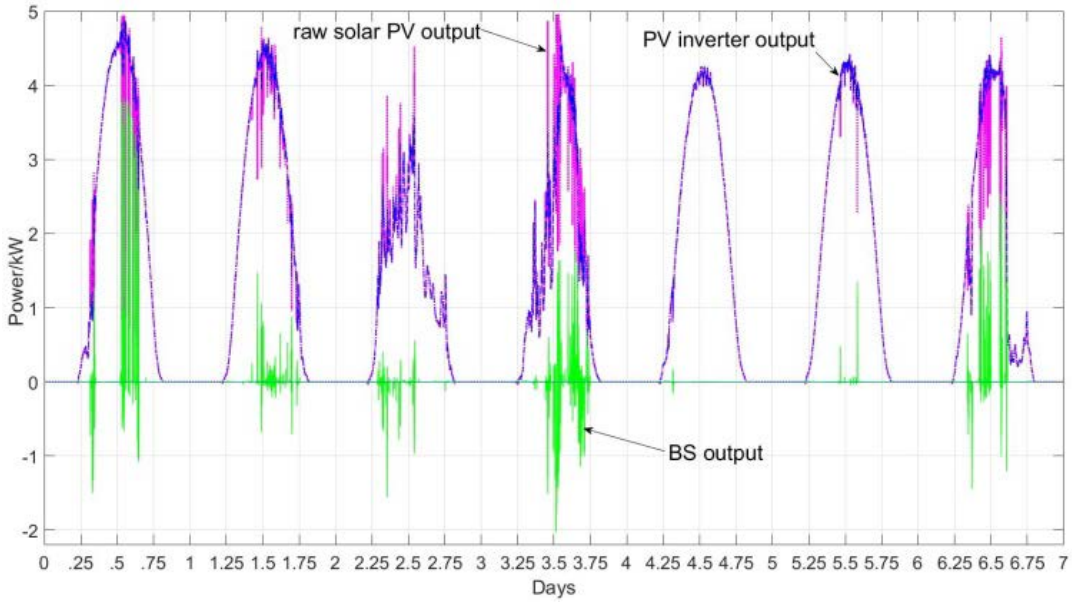

Figure 15: Solar PV output data, BESS output and inverter output with FF control

Fig. 15 depicts the raw solar PV output, BESS output and inverter output with FF control for week duration. Accordingly, Day 1 and 2 have the highest PV generation and variation articulates that these are sunny days with few clouds in the sky. Day 3 and 4 have largely varying PV generation and variation says that these are cloudy days. Day 5 and 6 have good PV generation and these are less sunny days than Day 1 and 2 but very few clouds in the sky. The pattern of the Day 7 shows that it has been a sunny day with more clouds until mid-day which turned to be an extremely cloudy afternoon. Fig. 15 proves that the proposed

FF control has been able to control the FF throughout the entire period with the integration of BESS.

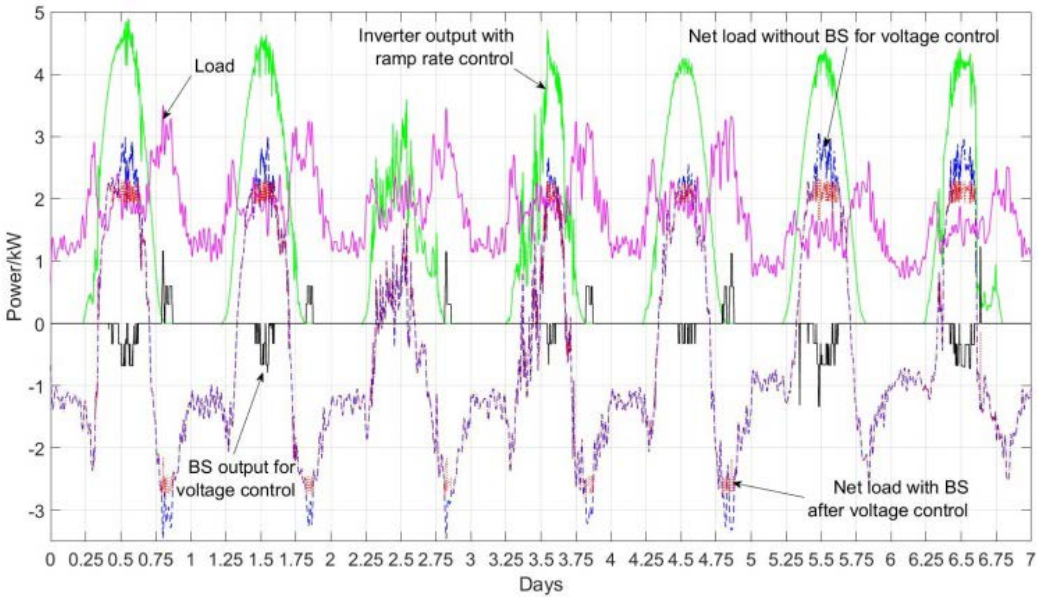

Figure 16: Inverter power with FF control, load demand, net power with/without BESS for FF control

Fig. 16 illustrates the inverter power output with FF control, the load demand, the net power with FF control with/without SF control. Accordingly, the BESS has been charged during mid-day for SF control during all the days except Day 3. Significantly less PV generation in the Day 3 caused no excess generation in the mid-day. The BESS has been discharged during evening peak period during all the days except Day 6 and 7 as a result of the fewer loads in weekend evenings. According to Fig. 16, the proposed methodology for voltage control has been able to control the voltage profile to lie within the operating voltage limits. Hence, the integrated controller for FF controller and the SF controller can be successfully implemented to alleviate fast and slow fluctuations in the voltage profile by integrating a BESS with the solar PV unit.

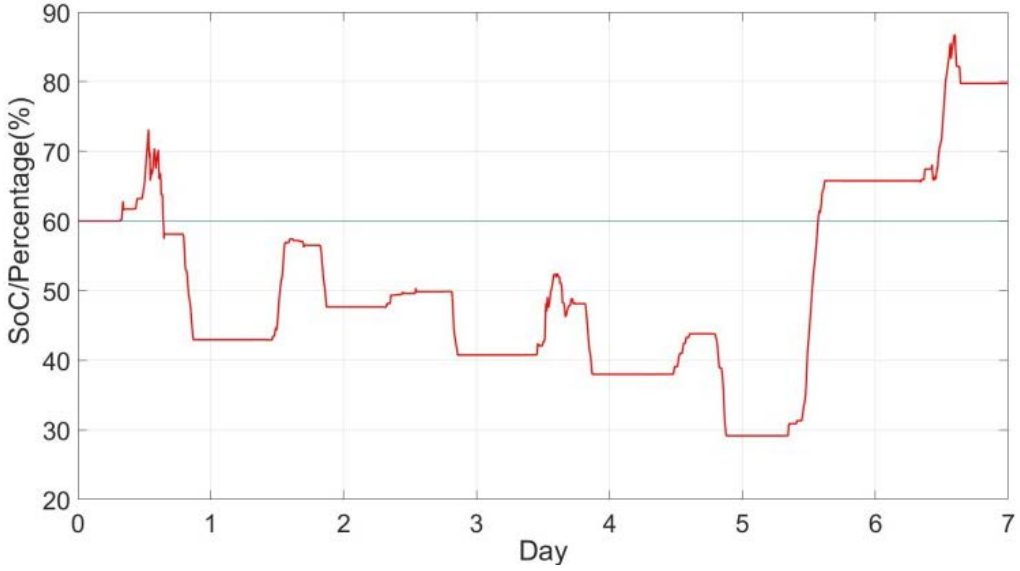

Figure 17: Overall variation of BESS SOC

Fig. 17 illustrates the SoC variation during entire duration (week) for SFVFC. Initial SoC is 60% and at the end of Day 1 SoC level has become 42%. SoC value had been 48%, 40%, 38%, 29%, 66% and 80% at the end of Day 2 - 7 respectively. The SoC management mechanism activates when the SoC become less than 30% or higher than 90% while the voltage at PCC meets the voltage requirement as per Table 3.

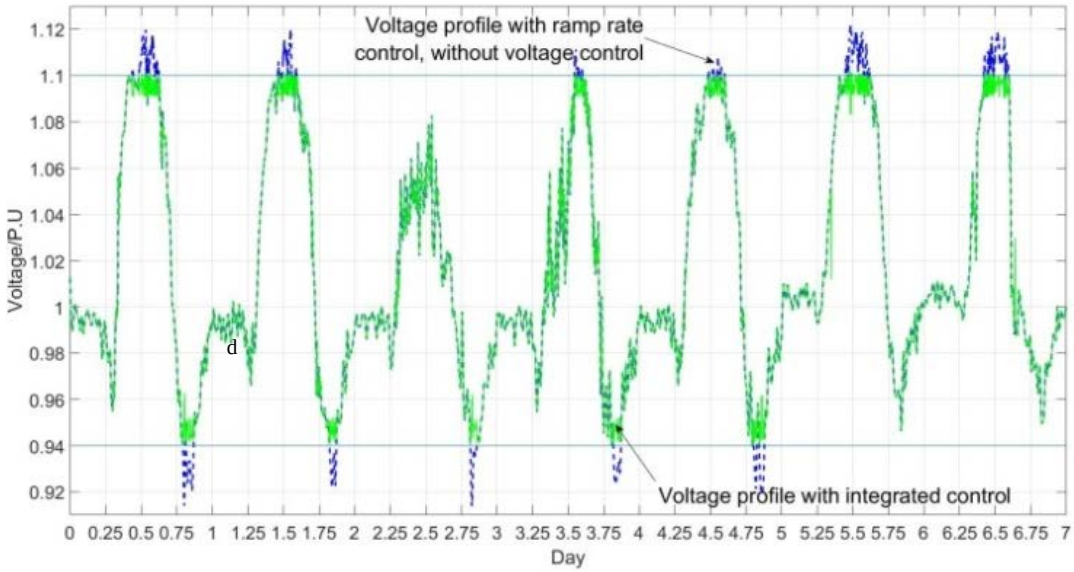

Figure.18: Voltage profile with FF control and with SFVFC

Fig. 18 shows the voltage profile in LV bus 16 with the FF controller only and with the proposed SFVFC. Accordingly, the voltage profile has been controlled within the operating voltage range while maintaining the rate of change of the solar PV inverter output at 5 watts/second maximum, Moreover, the simulations for the 7 day period strongly validate the successful implementation of the proposed integrated controller for SFVFC using a 500Ah lead acid BESS.

5. Conclusion

The application of a single BESS to alleviate the slow and fast fluctuations of solar PV output has been presented. The management of the battery SoC is included to ensure an undisrupted BESS support during the control. The SF has been alleviated by charging the BESS during mid-day, when the solar PV output is higher than the load demand and discharging the BESS during evening, when the solar PV output is absence and the load demand is high. The charging/discharging rate of BESS for the voltage control has been determined based on the voltage level at the PCC, which is a novel hypothesis that has not been reported in literature previously. Simultaneously, the FF control of the connected feeder has been achieved using the same BESS. The FF control mechanism proposed in this work is an original idea which has not been addressed in literature.

The control methodology presented in this work contributes to the industry through,

- Providing voltage control to mitigate both SF and FF simultaneously by dynamically calculating BESS output for every 1 second duration.
- Providing charge/discharge control methods to suit the power flow and BESS SoC.
- Opening up the discussion to provide incentives and tariff benefits to customers for supporting the grid.
- Introducing the variable charge/discharge methods to be implemented by the residential solar PV generator to conserve energy without curtailing the output power of the PV via inverter control, etc.

The proposed method is validated using a practical MV/LV network in NSW. The simulation results show that the proposed method can alleviate the slow (due to intermittency of solar PV) and the fast (due to passing cloud) fluctuations of the PV output. Initially, the specified rate of change of the inverter output (MARR), the operating voltage range and the severity levels are set, the method is not dependent on any simulation parameter thereafter. The proposed controller mechanism is tested using the same network for a 1 week period. The results show that the proposed methodology has effectively controlled the ramp rate of change of the inverter output while maintaining the voltage profile within the operating voltage range using a 500Ah lead acid BESS.

6. Acknowledgement

This work was supported by the Australian Research Council (ARC) grant LP100100618.

7. References

[1] J. Tant, F. Geth, D. Six, P. Tant and J. Driesen, "Multiobjective Battery Storage toImprove PV Integration in Residential Distribution Grids," in *IEEE Transactions on Sustainable Energy*, vol. 4, no. 1, pp. 182-191, Jan. 2013.

[2] M. Nassereddine, A. Hellany, M. Nagrial, J. Rizk and D. D. Micu, "Utilities investments into residential properties: PV solar system with energy storage," *2016 51st International Universities Power Engineering Conference (UPEC)*, Coimbra, 2016, pp. 1-4.

[3] K. Ananda-Rao, R. Ali, S. Taniselass and N. Baharudin, "Microcontroller based battery controller for peak shaving integrated with Solar Photovoltaic," *4th IET Clean Energy and Technology Conference (CEAT 2016)*, Kuala Lumpur, 2016, pp. 1-6.

[4] Neha Beniwal, Ikhlaq Hussain and Bhim Singh, " Control and operation of a solar PV-batterygrid-tied system in fixed and variable power mode", *IET Gener. Transm. Distrib., 2018, Vol. 12 Iss. 11, pp. 2633-2641*[5] N. Mahmud, A. Zahedi and A. Mahmud, "A Cooperative Operation of Novel PV Inverter Control Scheme and Storage Energy Management System Based on ANFIS for Voltage Regulation of Grid-Tied PV System," in *IEEE Transactions on Industrial Informatics*, vol. 13, no. 5, pp. 2657-2668, Oct. 2017.

[6] Joel Kennedy, Phil Ciufo, Ashish Agalgaonkar, “Voltage-based storage control for distributed photovoltaic generation with battery systems”, Journal of Energy Storage 8 (2016) 274–285

[7] S. Ghosh, S. Rahman and M. Pipattanasomporn, "Distribution Voltage Regulation Through Active Power Curtailment With PV Inverters and Solar Generation Forecasts," in *IEEE Transactions on Sustainable Energy*, vol. 8, no. 1, pp. 13-22, Jan. 2017.

[8] M. J. E. Alam, K. M. Muttaqi and D. Sutanto, "Mitigation of Rooftop Solar PV Impacts and Evening Peak Support by Managing Available Capacity of Distributed Energy Storage Systems," in *IEEE Transactions on Power Systems*, vol. 28, no. 4, pp. 3874-3884, Nov. 2013.

[9] M. J. E. Alam, K. M. Muttaqi and D. Sutanto, "Effective Utilization of Available PEV Battery Capacity for Mitigation of Solar PV Impact and Grid Support With Integrated V2G Functionality," in *IEEE Transactions on Smart Grid*, vol. 7, no. 3, pp. 1562-1571, May 2016.

[10] M. Zeraati, M. E. Hamedani Golshan and J. M. Guerrero, "Distributed Control of Battery Energy Storage Systems for Voltage Regulation in Distribution Networks With High PV Penetration," in *IEEE Transactions on Smart Grid*, vol. 9, no. 4, pp. 3582-3593, July 2018.

[11] Y. Wang, K. T. Tan, X. Y. Peng and P. L. So, "Coordinated Control of Distributed Energy-Storage Systems for Voltage Regulation in Distribution Networks," in *IEEE Transactions on Power Delivery*, vol. 31, no. 3, pp. 1132-1141, June 2016.

[12] H. R. Teymour, D. Sutanto, K. M. Muttaqi and P. Ciufo, "Solar PV and Battery Storage Integration using a New Configuration of a Three-Level NPC Inverter With Advanced Control Strategy," in *IEEE Transactions on Energy Conversion*, vol. 29, no. 2, pp. 354-365, June 2014.

[13] A. Chersin, W. Ongsakul and J. Mitra, "Improving of uncertain power generation of rooftop solar PV using battery storage," *2014 International Conference and Utility Exhibition on Green Energy for Sustainable Development (ICUE)*, Pattaya, 2014, pp. 1-4.

[14] R. P. Sasmal, S. Sen and A. Chakraborty, "Solar photovoltaic output smoothing: Using battery energy storage system," *2016 National Power Systems Conference (NPSC)*, Bhubaneswar, 2016, pp. 1-5.

[15] P. Ariyaratna, K. Muttaqi and D. Sutanto, "Novel methodology to simultaneously mitigate fast and slow voltage fluctuations of voltage profile in distribution feeder using

battery storage," *2017 Australasian Universities Power Engineering Conference (AUPEC)*, Melbourne, VIC, 2017, pp. 1-6.

[16] Prabha Ariyaratna, Kashem M. Muttaqi, Danny Sutanto, “A novel control strategy to mitigate slow and fast fluctuations of the voltage profile at common coupling Point of rooftop solar PV unit with an integrated hybrid energy storage system”, Journal of Energy Storage, Volume 20, 2018, Pg.409-417

[17] P. Ariyaratna, K. Muttaqi and D. Sutanto, "The sizing of battery energy storage for the mitigation of slow and fast fluctuations in rooftop solar PV output," *2017 IEEE Innovative Smart Grid Technologies - Asia (ISGT-Asia)*, Auckland, 2017, pp. 1-6

[18] C. A. Hill, M. C. Such, D. Chen, J. Gonzalez and W. M. Grady, "Battery Energy Storage for Enabling Integration of Distributed Solar Power Generation”, IEEE Transactions on Smart Grid, 2012, 3, (2), pp. 850-857.

[19] Ruifeng Yan and T. K. Saha, "Power ramp rate control for grid connected photovoltaic system”, Conference Proceedings IPEC, Singapore, 2010, pp. 83-88

[20] M. J. E. Alam, K. M. Muttaqi and D. Sutanto, "A Novel Approach for Ramp-Rate Control of Solar PV Using Energy Storage to Mitigate Output Fluctuations Caused by Cloud Passing”, IEEE Transactions on Energy Conversion, 2014,29,(2), pp. 507-518.

[21] I. de la Parra, J. Marcos, M. García and L. Marroyo, "Dynamic ramp-rate control to smooth short-term power fluctuations in large photovoltaic plants using battery storage systems," IECON 2016 - 42nd Annual Conference of the IEEE Industrial Electronics Society, Florence, 2016, pp. 3052-3057.

[22] J. Schnabel and S. Valkealahti, "Energy Storage Requirements for PV Power Ramp Rate Control in Northern Europe", *I*nternational Journal of Photoenergy, vol. 2016, pp. 1-11.

[23] W. Greenwood, O. Lavrova, A. Mammoli, F. Cheng, S. Willard, “Optimization Of Solar Pv Smoothing Algorithms For Reduced stress On A Utility-Scale Battery Energy Storage System”, Public Service Company of New Mexico (PNM), 2014

[24] George Hilton, Andrew Cruden, Jeremy Kent, “Comparative analysis of domestic and feeder connected batteries for low voltage networks with high photovoltaic penetration”, Journal of Energy Storage 13 (2017) 334–343

[25] F. Cheng, S. Willard, J. Hawkins, B. Arellano, O. Lavrova and A. Mammoli, "Applying battery energy storage to enhance the benefits of photovoltaics," IEEE Energytech, Cleveland, OH, 2012, pp. 1-5.

[26] R. Perez, "Lead-acid battery state of charge vs. voltage," Home Power, vol. 36, pp. 66-69, 1993